Journal of Applied Polymer Science

In Situ Preparation of Cyclohexanone Formaldehyde Resin/Layered Silicate Nanocomposites

Nilgün Kızılcan,[1,2] Mehmet Mermutlu[2]

[1]Department of Chemistry, Faculty of Science, Istanbul Technical University, Maslak 34469, Istanbul, Turkey

[2]Department of Nanoscience and Engineering, Graduate School of Science Engineering and Technology, Istanbul Technical University, Maslak 34469, Istanbul, Turkey

Correspondence to: N. Kızılcan (E-mail: kizilcan@itu.edu.tr)

ABSTRACT: In this study, *in situ* modified cyclohexanone formaldehyde resin (CFR) was prepared from clay (montmorillonite) and polydimethylsiloxane with diamine chain ends [α,ω-diamine poly(dimethyl siloxane) (DA.PDMS)] in the presence of a base catalyst. Different clay contents (from 0.5 to 3 wt %) were used to produce clay-modified nanocomposite ketonic resins [layered clay (LC)–CFR] and clay- and DA.PDMS-modified nanocomposite ketonic resins (DA.PDMS–LC–CFR). The polymeric nanocomposite material prepared by this method was directly synthesized in one step. These nanocomposites were confirmed from X-ray diffraction to have a layered structure with a folded or penetrated CFR, and they were further characterized via Fourier transform infrared spectroscopy–attenuated total reflectance and NMR spectroscopy. The thermal properties of all of the resins were studied with differential scanning calorimetry and thermogravimetric analysis. All of the resins showed higher thermal stability than their precursor CFR resin. The obtained samples were also characterized morphologically by scanning electron microscopy. © 2013 Wiley Periodicals, Inc. J. Appl. Polym. Sci. **2014**, *131*, 39918.

KEYWORDS: clay; composites; nanostructured polymers; resins

Received 8 February 2013; accepted 31 August 2013

DOI: 10.1002/app.39918

INTRODUCTION

Most commercial resins are generally solid materials with low molecular weight. They can also be processed easily. These types of resins are mainly used in surface coatings, varnishes, and inks and in the textile and paper industries as additive materials. Previous studies have demonstrated that the synthesis of copolymers of cyclohexanone formaldehyde resins (CFRs) with polydimethylsiloxane (PDMS) is possible by a one-step method of the *in situ* modification of a ketonic resin.[1] Polysiloxanes have many interesting properties, including high surface activities and low solubility parameters. These properties result in the thermodynamic incompatibility of polysiloxanes with most other organic polymer systems.[2–8] Siloxane-containing copolymers are used as compatibilizers along with organic polymers to overcome these difficulties. Siloxane segments of the copolymers migrate to the air–polymer surface in siloxane-containing copolymers, whereas the organic segments act as an anchoring group for the siloxane blocks, so that permanent surface modification can be obtained for the resins.

Since the late 1980s, nanoparticle-based polymer composites from Okada and colleagues[9] in the Toyota research group have attracted significant interest. They obtained enhanced properties for nylon 6/clay nanocomposites with *in situ* polymerization. The results of their study show that polymer nanocomposites based on layered silicates provide significant potential for the enhanced performance of polymer compounds. Until the early 2000s, there were few commercial materials available. These were mostly based on nylon 6. An increasing number of studies in this field has shown that many polymers, such as polyamide 6, can be used to obtain nanocomposites.[10–13] Nanocomposites obtained by organic polymers and inorganic clay minerals containing silicate layers such as montmorillonite (MMT), which belong to the family of 2:1 phyllosilicates, have attracted great interest because of the advantageous improvements in their mechanical, thermal, barrier, and clarity properties that are not possible with conventional fillers.[14–21] Polymer/layered silicate nanocomposites generally improve the properties of polymeric materials, even at very low volume fraction loadings (1–5%) of layered silicates; this is in contrast to the high volume fraction loading (>50%) in traditional advanced composites.[22] Nanometer-sized particles in a polymer/ceramic/metal matrix disperse to form nanocomposites. The polymers containing layered silicate clay minerals as a reinforcing agent can be classified

as speared (intercalated) or dispersed (exfoliated), depending on the dispersion of clay in the matrix. Hybrid organic–inorganic substances composed of nanometer-sized particles are dispersed in a polymer matrix that is known as a polymer/clay nanocomposite. Clays exhibit plastic behavior upon heating, and they remain hard at elevated temperatures. The distribution of inorganic materials in the polymer matrix is very important in the preparation of nanocomposites. The improper achievement of exfoliation causes clusters of inorganic materials in the polymer matrix, and this limits the improvement of their properties.[23,24] The improper achievement of exfoliation causes clusters of inorganic materials in the polymer matrix, and this limits the improvement of their properties.[24]

Polymeric composites and recently studied nanocomposites have received widespread attention because of profound improvements in the performance of polymers through the incorporation of microsized and nanosized fillers. Some of the important classes of nanoparticles used as fillers in polymeric composites consist of fumed silica, organoclays, carbon nanofibers, carbon nanotubes, titanium oxide, and very recently, graphene. Many polymers have been used as hosts for the preparation of composites based on such fillers.[25,26] Such composites have generally displayed highly improved thermal, mechanical, and engineering properties when compared with their virgin resins.

Contemporarily, there are many types of resin/clay nanocomposites, and progress is still being made day by day. The major types of resin/clay nanocomposites are epoxy resin/clay,[27] phenolic resin/clay,[24] and urea formaldehyde resin/clay nanocomposites.[28] Enhanced thermal, mechanical, and optical properties have been noted in research studies of these types of nanocomposites.

In this study, nanocomposites of CFR were synthesized by the direct addition of different contents (from 0.5 to 3 wt %) of clay into the synthesis media. During the synthesis, α,ω-diamine poly(dimethyl siloxane) (DA.PDMS) was also added to the media to improve the surface properties of the material. With this method, DA.PDMS-added polymeric nanocomposite materials were synthesized in one step. As a nanoscale material, layered silicate MMT clay was used for nanocomposite forms of *in situ* modified polydimethylsiloxane cyclohexanone formaldehyde resins. The final samples were studied with several characterization techniques to verify the structure of materials and their properties.

EXPERIMENTAL

Materials

Cyclohexanone and formaldehyde solution (37%) were supplied by Riedel-de Haen and LABSCAN, respectively, for the synthesis of the CFRs. Sodium hydroxide pellets were supplied by Riedel-de Haen. The nanofiller, sodium MMT (Nanofil 757), was provided from Süd-Chemie (Switzerland). The filler was a highly purified natural sodium MMT with a cation-exchange capacity of 80 mequiv/100 g, a medium of particle size (<10 μm), and a bulk density of approximately 2.6 g/cm^3. DA.PDMS was the product of Sigma-Aldrich (Germany) and had a molecular weight of 1000 ± 80.

Analysis

Fourier transform infrared (FTIR) spectra were obtained with a recording model PerkinElmer Spectrum One FTIR spectrophotometer with an attenuated total reflectance sampling accessory; they were obtained directly from the sample without KBr discs.

All ^{1}H-NMR data were obtained from a Varian (AC 500-MHz, Germany) spectrometer with CD_2Cl_2 as the solvent and tetra methyl silane (TMS) as the internal reference.

Differential scanning calorimetry (DSC) thermograms were obtained with a PerkinElmer DSC-6 instrument; the heating rate was 10°C/min starting from 30°C under a nitrogen atmosphere.

Thermogravimetric analysis (TGA) was carried out in a nitrogen atmosphere at a heating rate of 10°C/min up to 900°C in a PerkinElmer Pyris 1. The percentage weight loss of the samples was calculated in the temperature range of 20 to 800°C.

X-ray diffraction (XRD) results were obtained with a Rigaku D/Max-Ultima+/PC XRD instrument. The scanning rate was 10 to 70°.

The morphology of the products was examined by scanning electron microscopy (SEM; ESEM XL30 ESEM-FEG, Philips), and the samples for the SEM measurement were prepared by gold coating.

Preparation of the CFRs

Amounts of 98 g (1 mol) of cyclohexanone, 25 mL of cyclohexane, and 30 mL of 37% formalin were put into a three-necked flask equipped with a stirrer and a condenser. When the temperature of the mixture was raised to 70–80°C, refluxing was started, and subsequently, 100 mL of 37% formaline was added. As a catalyst, NaOH solution (20 wt %) was used. The reaction was further continued under pH values of 11–12 for 5 h. After the reaction time was completed, two layers were formed. We separated and purified the resin by decanting the water layer and washing it several times with warm water until it was free from it, and then, it was dried at 100°C in vacuum oven.

Preparation of the DA.PDMS-Modified CFR (DA.PDMS–CFR)

The preparation of CFRs was begun, and their modifier compounds (2 wt % DA.PDMS) were added to resin solution. The stirring was continued for 5 h more. After the reaction time was complete, two layers were formed. DA.PDMS-modified resin was recovered and purified as described earlier.

Preparation of the Layered Clay (LC)–CFR Nanocomposites

LC–CFR samples were synthesized in four different initially fed clay contents of several weight fractions (0.5, 1, 1.5, and 3 wt

Table I. Contents of the LC–CRF Nanocomposite Samples

Sample	Clay content (wt %)	C/F molar ratio
LC-CFR1	0.5	1:1.6
LC-CFR2	1	1:1.6
LC-CFR3	1.5	1:1.6
LC-CFR4	3	1:1.6

Table II. Contents of the DA.PDMS–LC–CRF Nanocomposite Samples

Sample	Clay content (wt %)	DA.PDMS content (wt %)	C/F molar ratio
DA.PDMS-LC-CFR1	0.5	2	1:1.6
DA.PDMS-LC-CFR2	1	2	1:1.6
DA.PDMS-LC-CFR3	1.5	2	1:1.6
DA.PDMS-LC-CFR4	3	2	1:1.6

%). The unmodified MMT (pristine) clay was used to prepare the resin/clay nanocomposites. The preparation of CFRs was begun, and the desired clay content was added to the resin solution. The stirring continued for 5 h more. After the reaction time was complete, two layers were formed. Nanocomposite resin was recovered and purified as described earlier. The final samples were named with reference to their clay contents. The clay contents of the resin samples are given in Table I.

Preparation of the DA.PDMS–LC–CFR Nanocomposites

The DA.PDMS–LC–CFR samples were synthesized with four different initial feed clay contents by weight (0.5, 1, 1.5, and 3 wt %). Unmodified MMT clay was used to prepare the resin/clay nanocomposites. The preparation of the DA.PDMS-modified CFR was begun, and the desired clay content was added to the resin solution. The stirring was continued for 5 h more. After the reaction time was complete, two layers were formed. Nanocomposite resin was recovered and purified as described earlier. The final samples were named with reference to their clay contents. The clay and PDMS contents of the resin samples are given in Table II.

RESULTS AND DISCUSSION

Four pristine LC–CFRs and four DA.PDMS–LC–CFRs were synthesized with weight percentages of 0.5, 1, 1.5, and 3 wt % with one step. The constant ratio of monomers (cyclohexanone/formaldehyde) was 1:1.6, and a constant amount of DA.PDMS of 2 wt % was applied in each polymerization reaction of the resins.

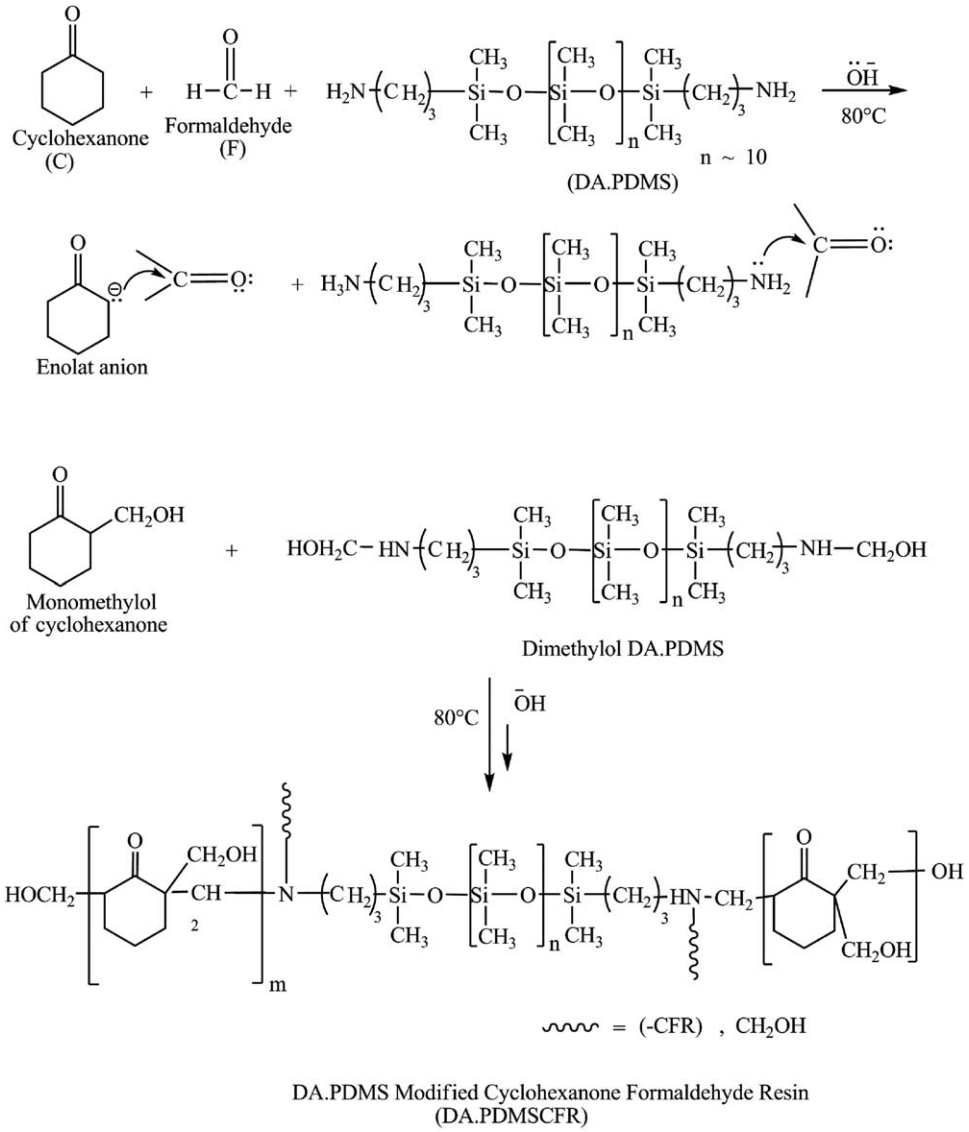

Scheme 1. Formation of the DA.PDMS–LC–CFR nanocomposites.

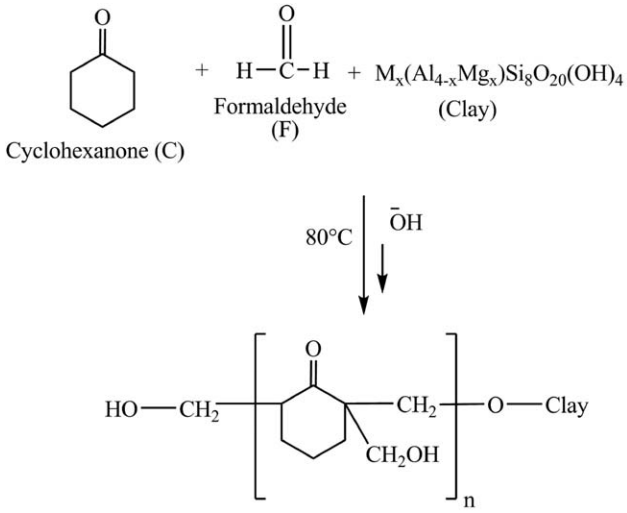

Scheme 2. Formation of the LC–CFR nanocomposite.

The formation of the CFRs started with an aldol-like reaction after the base-catalyzed elimination reaction of water from the methylol derivatives of cyclohexanone. In the DA.PDMS-modified CFRs, PDMS molecules with an amine chain end probably acted as an amine component of a Mannich-type reaction under the resin preparation conditions. Because the molar ratio of formaldehyde to amine was rather high, each $-NH_2$ group should have reacted with 2 mol of formaldehyde and 2 mol of ketone. The intermediates formed from aldol-like reactions and Mannich-type reactions and, combined with the effect of the base catalyst, formed modified resin similar to base-catalyzed ketonic resins.[1] Pristine layered silicates usually contain hydrated Na^+ or K^+ ions. Obviously, in this pristine state, layered silicates are only miscible with hydroxyl groups on the ketonic resin. To render layered silicates miscible with other polymer matrices, one must convert the normally hydrophilic silicate surface to an organophilic one and make the intercalation of many engineering polymers possible. Generally, this can be done by the reaction of the hydroxyl groups of pristine clay with the formaldehyde or methylol groups of ketonic resin. The formation of DA.PDMC–CFR, LC–CFR, and DA.PDMS–LC–CFR are shown in Schemes 3–1.

To characterize the chemical structures of the CFRs and DA.PDMS–CFRs, the MMT (pristine clay), LC–CFR1, LC–CFR2, LC–CFR3, LC–CFR4, DA.PDMS–LC–CFR1, DA.PDMS–LC–CFR2, DA.PDMS–LC–CFR3, and DA.PDMS–LC–CFR4 samples were analyzed with FTIR spectroscopy. Characteristic peaks of the CFRs appeared at 3400, 2920, 1700, and 1450 cm^{-1}. In this study, these characteristic peaks were observed at 3399, 2925, 1699, and 1445 cm^{-1}. These peaks were attributed to hydroxyl methyl groups, aliphatic $-CH_2$, carbonyl C=O, and $-CH_2$ methylene bridges, respectively. Also, between 970 and 1200 cm^{-1}, three main peaks were observed, which belonged to the C—O stretching between methylene bridges and cyclohexanone rings. In addition to these values, when we examined DA.PDMS–CFR, a peak at 860 cm^{-1} and an increase in the absorbance level at 1000–1100 cm^{-1} were observed. These peaks belonged to $Si-CH_3$ groups and Si—O—Si groups, respectively. Because of the —CO vibrations between 1150 and 750 cm^{-1}, these $Si-CH_3$

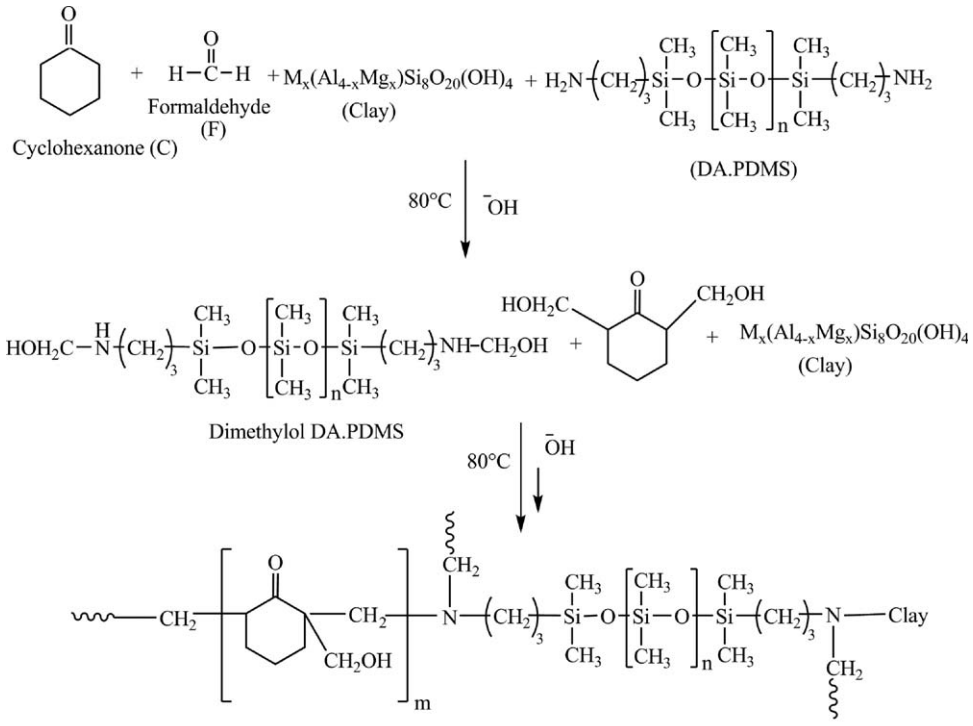

Scheme 3. Formation of DA.PDMS–CFR.

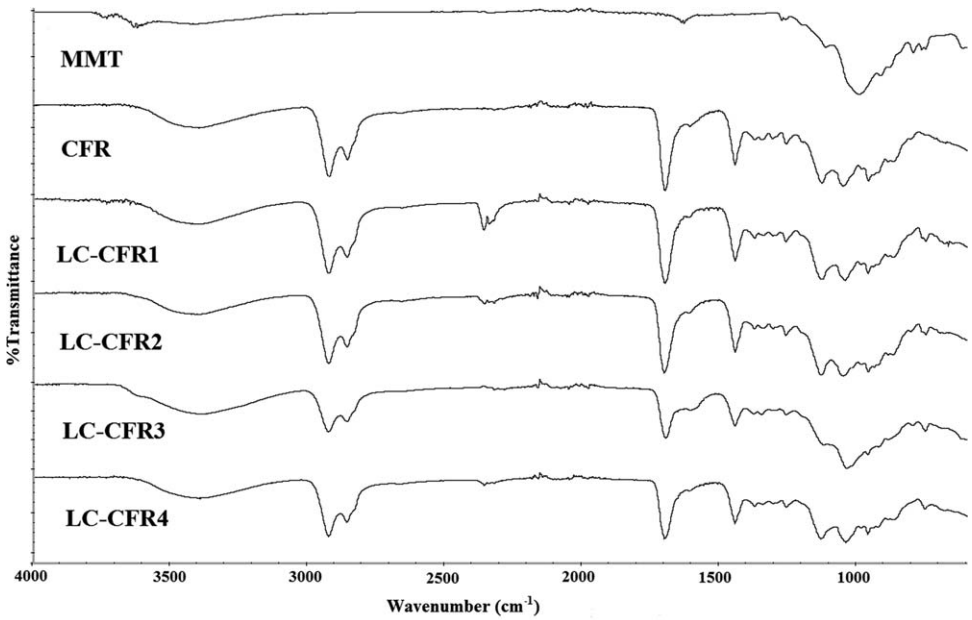

Figure 1. FTIR spectra of the pristine clay, CFR, and LC–CFRs.

and Si—O—Si vibrations were barely noticeable on the spectrum. The FTIR spectra of the pristine clay, CFR, DA.PDMS–CFR, and nanocomposite resins and both LC–CFRs and DA.PDMS–LC–CFRs are given in Figures 1 and 2, respectively. The main differences appeared at 747–756 and 1041–1051 cm^{-1} because of the Si—O deformation in MMT and Si—O—Si strength in both MMT and PDMS. As we mentioned, —CO vibrations between 1150 and 750 cm^{-1} and Si—O—Si vibrations were barely noticeable on the spectrum, but the intensity strengthened with increasing amount of MMT in the nanocomposites.

The ^{1}H-NMR spectra were recorded from the deuterated solvent solution, which was CD_2Cl_2. The spectra of CFR and DA.PDMS–CFR are shown in Figure 3. The peaks that appeared at 1.1–2.4 ppm were due to the aliphatic —CH_2 and —CH groups, those between 3.2 and 4.2 ppm were due to the —CH_2 methylene bridges and methyl groups, and those between 4.5 and 4.8 ppm due to the —OH groups of the methyl groups. Also, the peaks at 0.05–0.1 ppm were due to —Si—CH_2 and Si—CH_3 groups, and those at 0.9–1 ppm were due to —NH groups and appeared because of DA.PDMS.

The glass-transition temperature (T_g) values of the nanocomposite resins were examined by DSC in the range 30–300°C at a 10°/min heating rate. The DSC measurements of CFR, DA.PDMS–CFR, LC–CFR1, LC–CFR2, LC–CFR3, LC–CFR4, DA.PDMS–LC–CFR1, DA.PDMS–LC–CFR2, DA.PDMS–LC–CFR3, and DA.PDMS–LC–CFR4 were performed for one cycle.

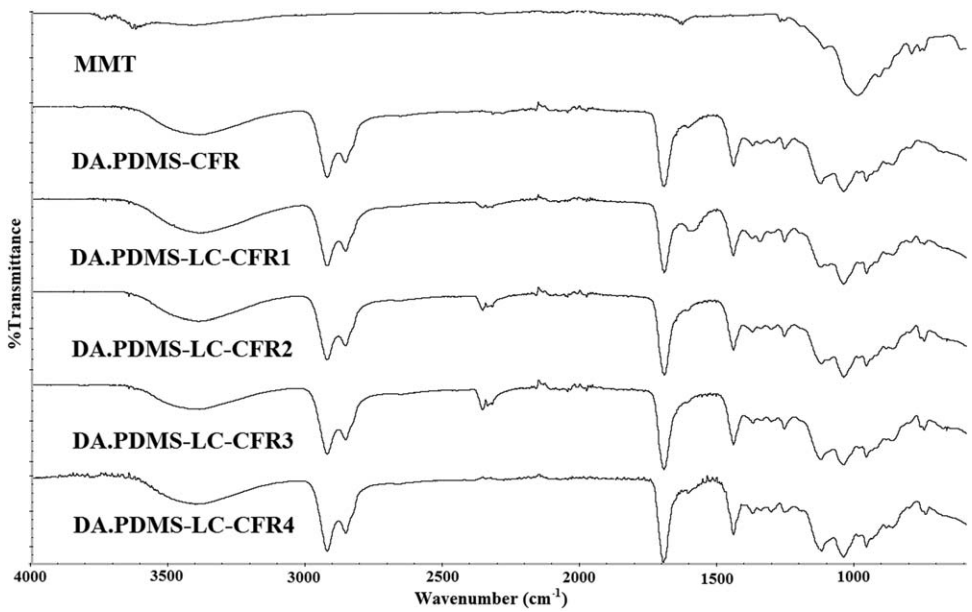

Figure 2. FTIR spectra of the pristine clay, DA.PDMS–CFR, and DA.PDMS–LC–CFRs.

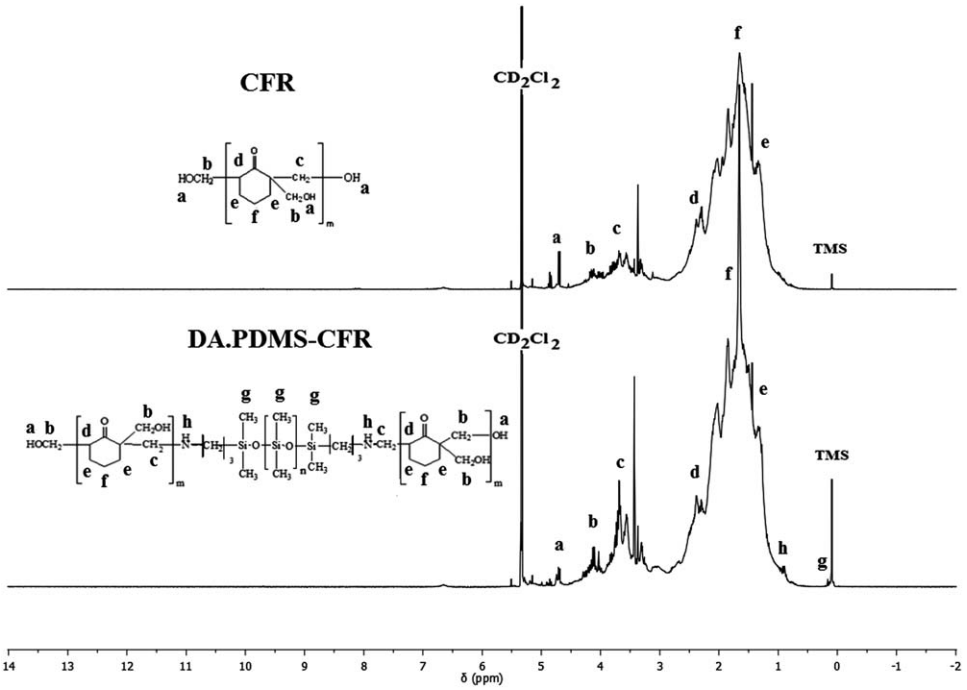

Figure 3. ^{1}H-NMR spectra of the CFR and DA.PDMS–CFR.

As shown in Figure 4, the T_g values of the CFR, LC–CFR1, LC–CFR2, and LC–CFR3 samples were determined to be 45, 60, 61, and 68°C, respectively. Also when we looked at the results of the DA.PDMS–LC–CFRs in Figure 5, the T_g values of DA.PDMS–CFR, DA.PDMS–LC–CFR1, DA.PDMS–LC–CFR2, DA.PDMS–LC–CFR3, and DA.PDMS–LC–CFR4 samples were determined to be 68, 119, 113, 117, and 122°C, respectively. These values are also given in Table III. In the view of such information, the T_g values of the nanocomposite resin samples increased with increasing clay content (in weight percentage).

The thermal decomposition behavior of the neat CFR, LC–CFRs, DA.PDMS–CFRs, and DA.PDMS–LC–CFRs were determined via TGA measurements. Degradation was carried out in a static air atmosphere to a maximum temperature of 800°C. The onset temperature of degradation (in degrees Celsius), the temperature at 50% residue amount and percentage residue amount at 500°C were calculated, and these values are given in Table III.

As shown in Figures 6 and 7, different stages of degradation occurred. In the first stage (up to 350°C) formaldehyde was released, and methylene bridges were broken. Then, in the second stage of decomposition, oxidation of the network occurred. In particular, for the amount of 3 wt % MMT addition,

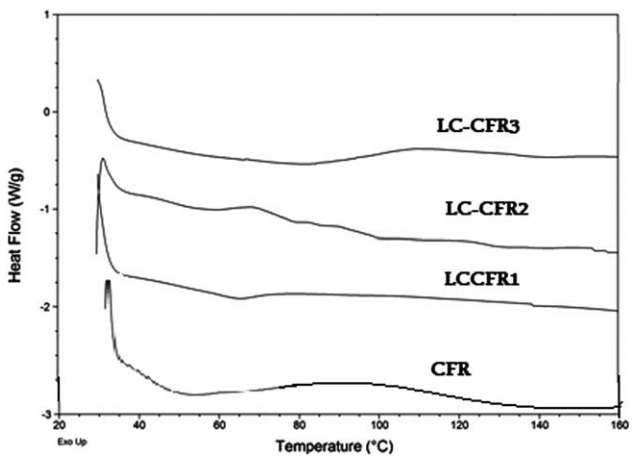

Figure 4. DSC thermograms of the CFR and LC–CFRs.

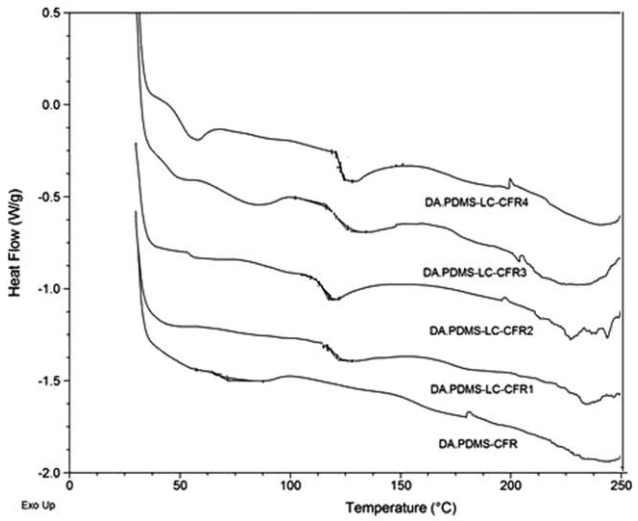

Figure 5. DSC thermograms of the DA.PDMS–CFR and DA.PDMS–LC–CFRs.

Table III. DSC and TGA Results for the CFR, DA.PDMS–CFR, LC–CFRs, and DA.PDMS–LC–CFRs

Sample	T_g (°C)[a]	Onset temperature of degradation (°C)[b]	$T_{50\%}$ (°C)[b]	Residue at 500°C (%)[b]
CFR	45	141	344	2,1
LC-CFR1	60	143	328	2,3
LC-CFR2	61	148	350	2,3
LC-CFR3	68	152	352	2,6
LC-CFR4	—	164	338	9,8
DA.PDMS-CFR	68	144	336	2,4
DA.PDMS-LC-CFR1	119	151	337	2,4
DA.PDMS-LC-CFR2	113	156	336	2,1
DA.PDMS-LC-CFR3	117	166	352	2,2
DA.PDMS-LC-CFR4	122	150	336	2,5

$T_{50\%}$, 50% weight loss temperature.
[a] Detected by DSC.
[b] Detected by TGA.

refracting due the agglomeration of MMT particles was observed, but we could clearly see that the addition of clay to the resin media helped to improve the thermal resistance of the neat CFR and DA.PDMS–CFR.

2θ measurements and d_{001} spacings (Å) (where d_{001} is interlayer distance, d-spacing in the direction of lattice plane diffraction peak (001)) of the final samples are given in Table IV. The d_{001} spacings (Å) were calculated with the Bragg equation with the help of the obtained 2θ measurement values. The 2θ value of the neat MMT clay used was found to be 7.3°. As shown in Figure 8, 2θ values shifted 2θ degrees lower in comparison with pristine clay. In this case, the interlayer space was increased from 12 to 16 Å and from 12 to 15 Å for the LC–CFRs and DA.PDMS–LC–CFRs, respectively. The results indicate that the interlayer spacing of the pristine clay was increased significantly by a one-step process, and these results show that the intercalation of the clay molecules in the resin media was successfully achieved.

SEM images of the LC–CFRs and DA.PDMS–LC–CFRs are shown in Figures 9 and 10, respectively. As shown in these figures, embedded nanoclay particles were observed on the sample surfaces. At a magnification of 15,000×, a homogeneous dispersion of clay particles could be seen. Also, at a magnification of 50,000× or higher, angled clay particles became visible. In addition, microvoids due to the curing of the byproduct of water molecules released during the polymerization reaction were observed.

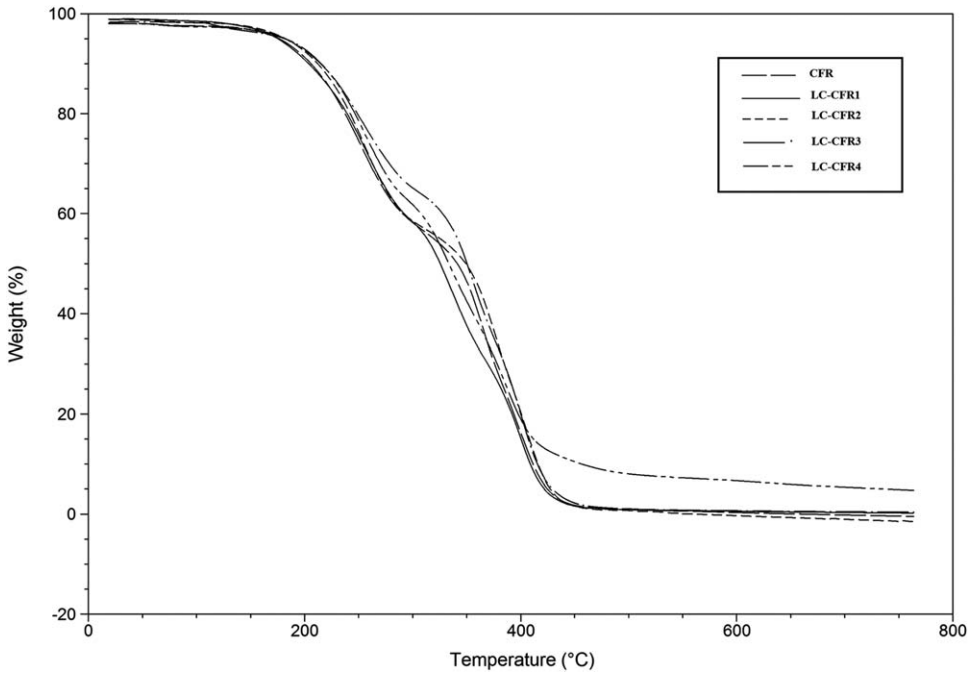

Figure 6. TGA thermograms of the CFR and LC–CFRs.

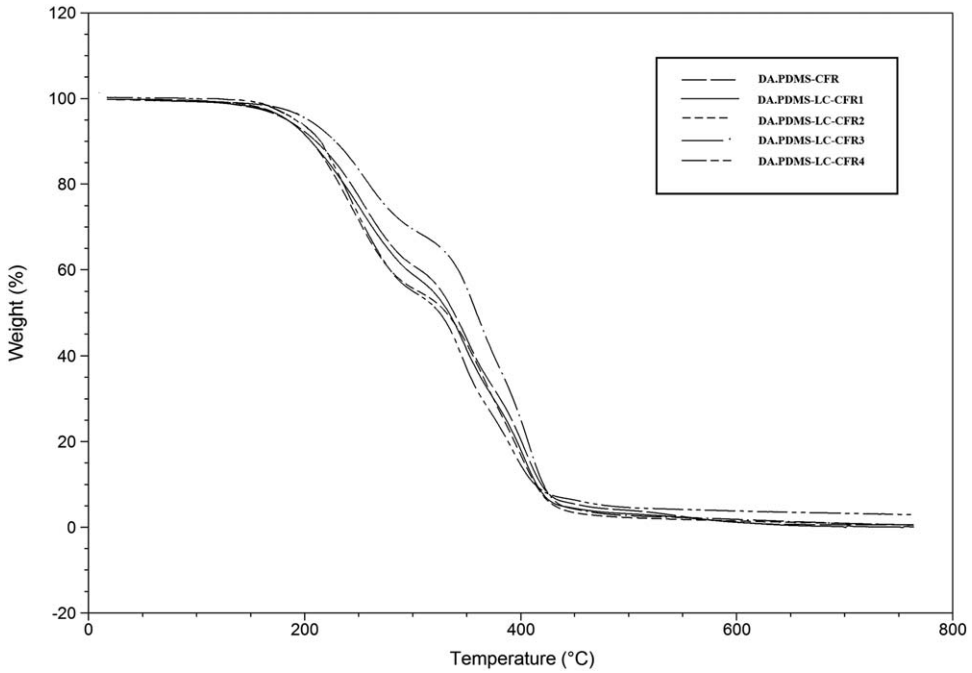

Figure 7. TGA thermograms of the DA.PDMS–LC–CFR and DA.PDMS–LC–CFRs.

Table IV. Interlayer Spacing of the Resin Nanocomposites

Sample	Additive (wt % of clay)	2θ (°)	d_{001} (Å)
Pristine clay	—	7.3	12
LC-CFR1	0.5	6.0	15
LC-CFR2	1	6.0	15
LC-CFR3	1.5	5.7	15
LC-CFR4	3	5.6	16
DA.PDMS-LC-CFR1	0.5	6.7	13
DA.PDMS-LC-CFR2	1	6.2	14
DA.PDMS-LC-CFR3	1.5	6.1	14
DA.PDMS-LC-CFR4	3	5.9	15

The homogeneous dispersal of clay particles was smoothly achieved for samples with clay contents of 0.5, 1, and 1.5 wt %. However, above a content of 1.5 wt %, as shown in Figures 9(g,h) and 10(g,h), the agglomeration of clay particles occurred. A high surface energy of nanoparticles forced them to agglomerate and form clay tactoids. Therefore, samples with clay contents higher than 1.5 wt % had problems with homogeneous dispersal. Dispersion could be improved with techniques such as high shear mixing and ultrasonication. Also, the modification of pristine clay may help better disperse clay particles in resin media.

CONCLUSIONS

The FTIR and ^{1}H-NMR results of the final samples indicate that copolymers of PDMS cyclohexanone formaldehyde and

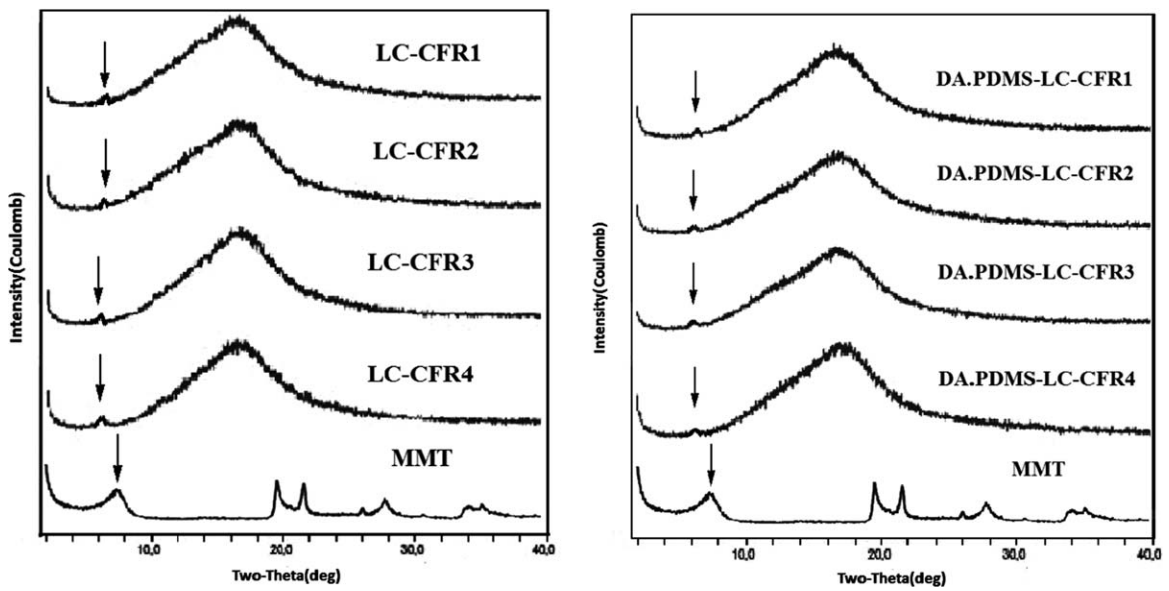

Figure 8. XRD patterns of the LC–CFRs and DA.PDMS–LC–CFRs.

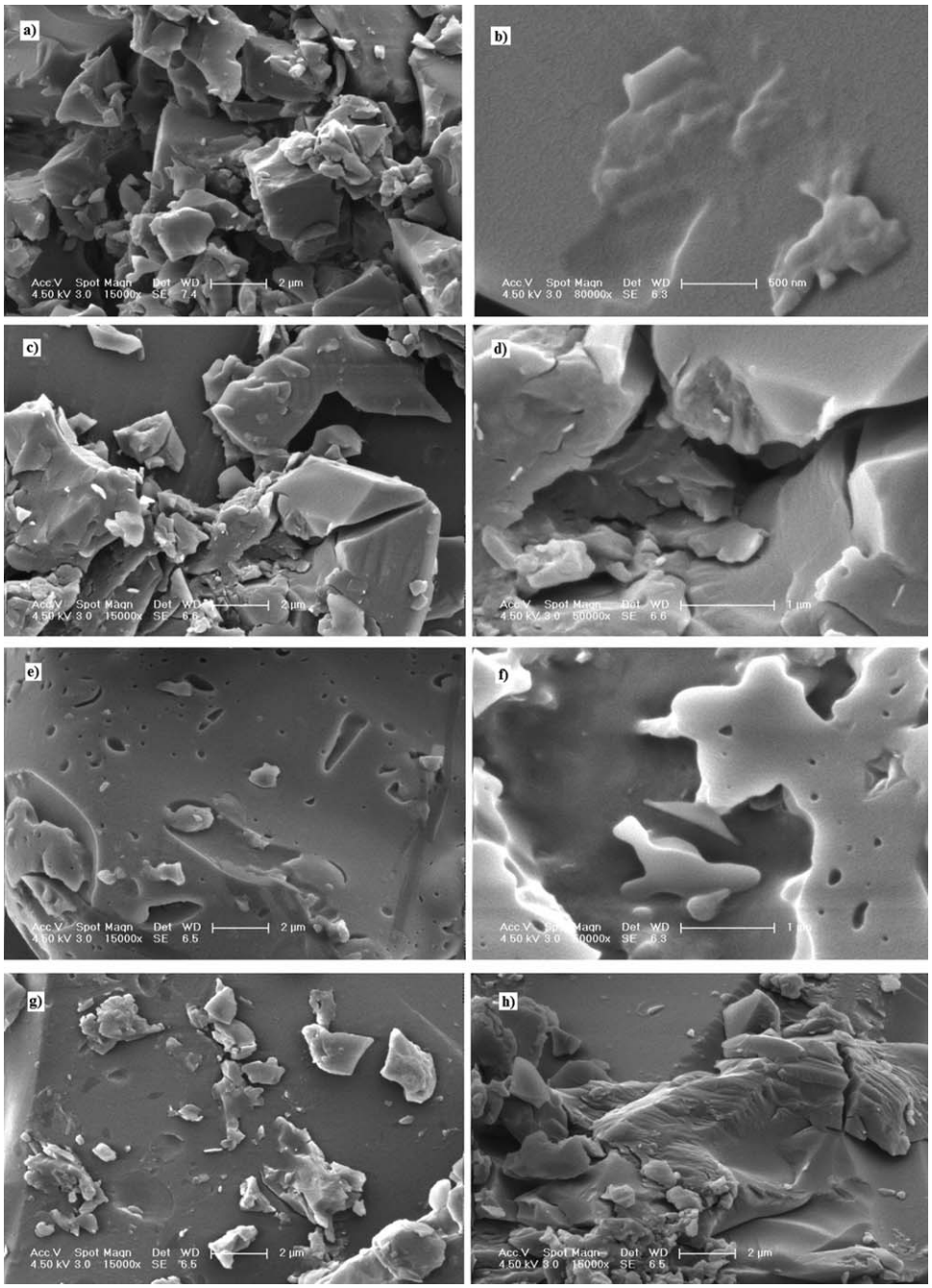

Figure 9. SEM images of the LC–CFRs.

nanocomposites forms of the resin samples were successfully synthesized with a one-step process. When we looked at the thermal analysis results, the T_g's and heat resistance levels of the final samples were clearly shown to increase with the addition of PDMS and MMT clay to the resin media. Increased levels were determined with these results, and they were used in explaining the conditions in detail. To determine the basal spacing of the MMT clay in the resin media, XRD analysis were used, and the results show that the interlayer spacing of pristine clay increased significantly. These results show that the intercalation of clay molecules in the resin media was successfully achieved. Also, the homogeneous dispersion of clay was observed in SEM images up to a weight percentage of clay 1.5 wt %, and above this percentage, clay tactoids due to the agglomeration of clay nanoparticles were observed. The determining factor of clay content was agglomeration; this was about 1.5 wt % content of clay in the resin media.

This study showed that as a ketonic resin, cyclohexanone formaldehyde could be synthesized as a form of nanocomposite with the direct addition of clay nanoparticles to the resin media; also, all known resin/layered silicate nanocomposites, such as epoxy or phenolic resins, could be reacted to become nanocomposites with this one-step *in situ* modification process.

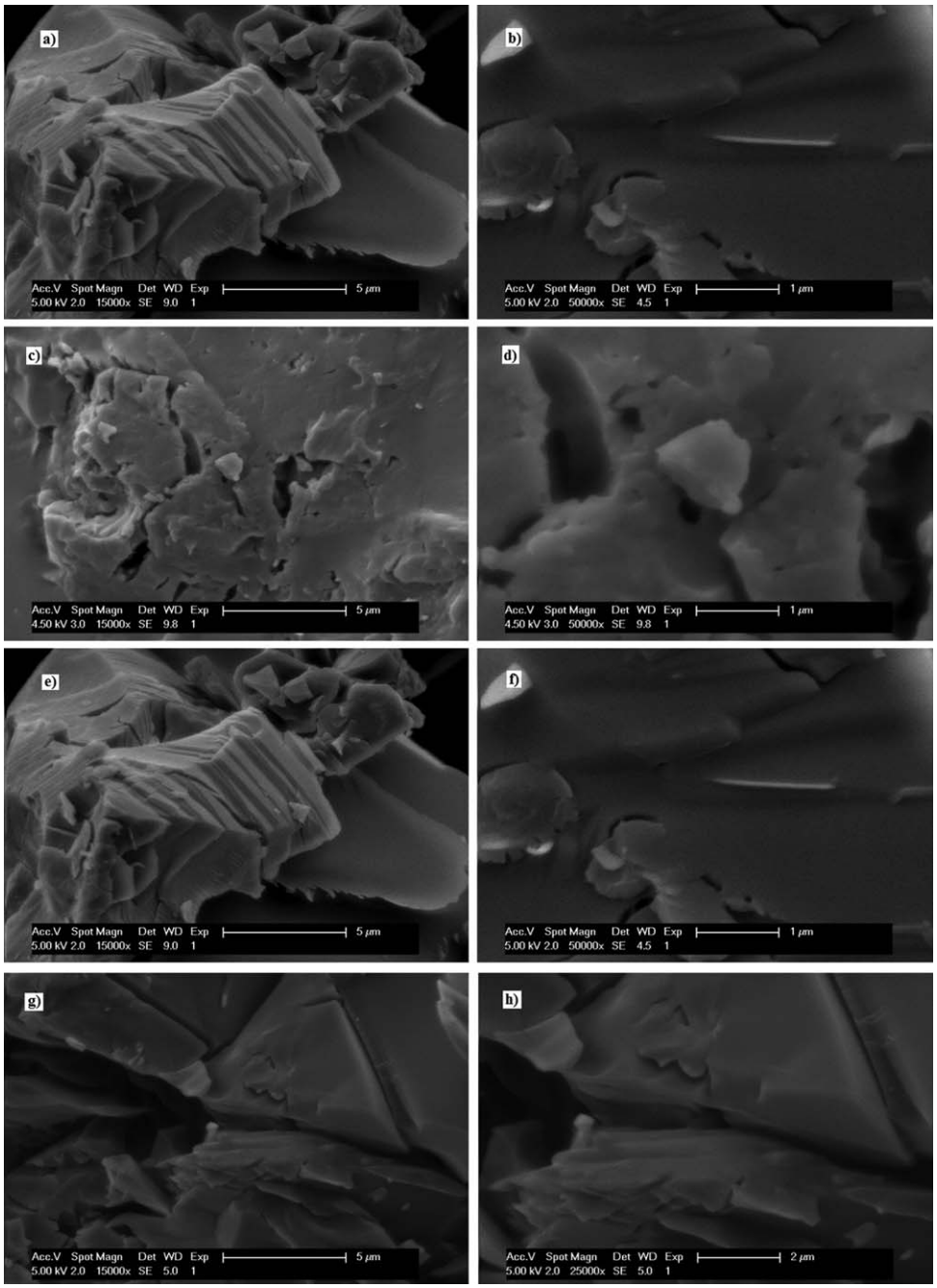

Figure 10. SEM images of the DA.PDMS–LC–CFRs.

REFERENCES

1. Kızılcan, N.; Akar, A. *J. Appl. Polym. Sci.* **2005**, *98*, 97.
2. Uyanık, N.; Yalçınkaya, H.; Kızılcan, N. *Surf. Coat. Int. Part B* **2001**, *84*, 309.
3. Kızılcan, N.; Ustamehmetoğlu, B.; Öz, N.; Saraç, S.; Akar, A. *J. Appl. Polym. Sci.* **2003**, *89*, 2896.
4. Kızılcan, N.; Öz, N.; Ustamehmetoğlu, B.; Akar, A. *Eur. Polym. J.* **2006**, *42*, 2361.
5. Kızılcan, N.; Öz, N.; Ustamehmetoğlu, B.; Akar, A. *Eur. Polym. J.* **2009**, *45*, 1857.
6. Akar, A.; Kızılcan, N.; Ustamehmetoğlu, B.; Çolak, D.; Saraç, S.; Çolak, C. *J. Appl. Polym. Sci.* **2007**, *106*, 3694.
7. Ustamehmetoğlu, B.; Kızılcan, N.; Demir, Ö. *Pigment Resin Technol.* **2012**, *41*, 179.
8. Köken, N.; Karagöz, S.; Kızılcan, N.; Ustamehmetoğlu, B. *J. Appl. Polym. Sci.* **2013**, *127*, 3790.
9. Yano, K.; Usuki, A.; Okada, A.; Kurauchi, T.; Kamigaito, O. *J. Polym. Sci. Part A: Polym. Chem.*, **1993**, *31*, 2493.
10. Giannelis, E. P. *Adv. Mater.***1996**, *8*, 29.
11. Lan, T.; Pinnavaia, T. *J. Chem. Mater.* **1994**, *6*, 2216.

12. Shi, H.; Lan, T.; Pinnavaia, T. *J. Chem. Mater.* **1996**, *8*, 1584.
13. Wang, Z.; Pinnavaia, T. *J. Chem. Mater.* **1998**, *10*, 3769.
14. Usuki, A.; Kawasumi. M.; Kojima, Y. *J. Mater. Res.* **1993**, *8*, 1174.
15. Lee, S. M.; Hwang, T. R.; Lee, J. W. *Polym. Eng. Sci.* **2004**, *44*, 1170.
16. Chen, B.; Evans, J. R. G. *Polym. Int.* **2005**, *54*, 807.
17. Garcıa-Lopez, D.; Gobernado-Mitre, I.; Fernandez, J. F.; Pastor, J. M. *Polymer* **2005**, *46*, 2758.
18. Tortora, M.; Gorrasi, G.; Vittoria, V.; Chiellini, E. *Polym. J.* **2002**, *43*, 6147.
19. Becker, O.; Varley, R.; Simon, G. *Polymer* **2002**, *43*, 4365.
20. Liu, T. X.; Liu, Z. H.; Ma, K. X.; He, C. B. *Compos. Sci. Technol.* **2003**, *63*, 331.
21. McNally. T.; Murphy, W. R.; Lew, C. Y.; Brennan, G. P. *Polymer* **2003**, *44*, 2761.
22. Dubois, P.; Alexandre, M. *Mater. Sci. Eng.* **2000**, *28*, 1.
23. Zhang, Z.; Ye, G.; Toghiani, H. *Macromol. Mater. Eng.* **2010**, *295*, 923.
24. Özkaraman, G.; Kızılcan, N. *J. Appl. Polym. Sci.* **2013**, *129*, 2966.
25. Yilgor, E.; Eynur, T.; Kosak, C.; Bilgin, S.; Yilgor, I.; Malay, O.; Menceloğlu, Y.; Wilkes, L. G. *Polymer* **2011**, *52*, 4189.
26. Li, H.; Gao, D.Y. *Pigment Resin Technol.* **2011**, *40*, 79.
27. Becker, O.; Varley, R.; Simon, G. *Polymer* **2002**, *43*, 4365.
28. Ateş, E.; Uyanık, N.; Kızılcan, N. *Pigment Resin Technol.* **2013**, *42*, 283.